

Hartmut Frey · Hamid R. Khan *Editors*

Handbook of Thin-Film Technology

 Springer

Handbook of Thin-Film Technology

Hartmut Frey · Hamid R. Khan
Editors

Handbook of Thin-Film Technology

 Springer

Editors

Prof. Dr. Hartmut Frey
Esslingen, Germany

Prof. Dr. Hamid R. Khan
Schwäbisch Gmünd, Germany

ISBN 978-3-642-05429-7

ISBN 978-3-642-05430-3 (eBook)

DOI 10.1007/978-3-642-05430-3

Library of Congress Control Number: 2015934012

Springer

© Springer-Verlag Berlin Heidelberg 2015

This work is subject to copyright. All rights are reserved, whether the whole or part of the material is concerned, specifically the rights of translation, reprinting, reuse of illustrations, recitation, broadcasting, reproduction on microfilm or in any other way, and storage in data banks. Duplication of this publication or parts thereof is permitted only under the provisions of the German Copyright Law of September 9, 1965, in its current version, and permission for use must always be obtained from Springer. Violations are liable to prosecution under the German Copyright Law.

The use of general descriptive names, registered names, trademarks, etc. in this publication does not imply, even in the absence of a specific statement, that such names are exempt from the relevant protective laws and regulations and therefore free for general use.

Printed on acid-free paper

Springer-Verlag GmbH Berlin Heidelberg is part of Springer Science+Business Media
(www.springer.com)

Acknowledgement

Thin film technology has become an engine for innovation in the computer- and networking industry. The alternative energy and the emission-free drives for vehicles, based also on the thin film technology. The Handbook of Thin-Film Technology presents a collection of current knowledge on coating technologies and their applications. Additionally methods for determining the properties of thin films are also covered. We are very grateful to Mrs. Dipl.-Ing. Carmen Frey for preparing and drawing the figures of this book. We would also like to thank the Management and Staff of Springer Publishing Company, for their support and cooperation.

Contents

1	Applications and Developments of Thin Film Technology . . .	1
	<i>by H. Frey</i>	
2	Relevance of the Vacuum Technology for Thin Film Coatings	5
	<i>by H. Frey</i>	
2.1	Introduction	5
2.2	Influence of Residual Gas on Film Quality	5
2.3	Generation of Vacuum	7
2.4	Vacuum Measurement	10
2.4.1	Thermal Conductivity Gauge	10
2.4.2	Friction Vacuum Gauge	11
2.4.3	Cold Cathode Ionization Vacuum Gauge	11
2.4.4	Hot-Cathode Ionization Gauge	11
2.4.5	Total Pressure Measurement in Coating Processes	11
2.4.6	Partial Pressure Measurement	12
3	Vacuum Evaporation	13
	<i>by H. Frey</i>	
3.1	Introduction	13
3.2	Fundamentals	13
3.2.1	Evaporation Processes	13
3.2.2	Transport Phase	15
3.2.3	Condensation Phase	16
3.3	Evaporation of Different Materials	17
3.3.1	Chemical Elements	17
3.3.2	Alloys	18
3.3.3	Compounds	26
3.4	Vapour Distribution	29
3.4.1	Small Surface Evaporators	29
3.4.2	Evaporation Arrangements with Expanded Source Distribution	33
3.4.3	Vapour Propagation with Small Free Path Length	34
3.5	Equipment Technology	37
3.5.1	Prefaces	37
3.5.2	Auxiliary Equipment for Evaporation Plants	38
3.5.3	Electron Emission	44
3.5.4	Evaporation Rate	53

3.6	Ion Plating	62
3.6.1	Characterization of Ion Plating	62
3.6.2	Influence on the Film Characteristics and Consequences for the Coating Process	64
3.6.3	Equipment for Ion Plating	64
3.6.4	Structural Constitution of the Ion Plated Films	66
3.6.5	Adhesive Strength of Ion Plated Films	68
3.6.6	Reactive Ion Plating	68
4	Basic Principle of Plasma Physics	73
	<i>by H. Frey</i>	
4.1	Introduction	73
4.2	Quasi-Neutrality	73
4.3	Characteristic Quantities	75
4.3.1	Langmuir Plasma Frequency	75
4.3.2	Debye Shielding Length	75
4.3.3	Landau Length and Plasma Parameters	76
4.4	Motion of Charged Particles in Electromagnetic Fields	77
4.4.1	Maxwell Equations	77
4.4.2	Equation of Motion and Law of Conservation of Energy	78
4.4.3	Larmor Motion	79
4.5	Collision Determined Plasmas	80
4.5.1	Distribution of Velocity	80
4.5.2	Mean Free Path and Collision Frequencies	82
4.5.3	Drift Motion of Charge Carriers in an Electrical Field with Consideration of Collisions	83
4.5.4	Ionization and Recombination	85
4.5.5	Plasma as Continuum	91
4.5.6	Transportation Processes	102
4.6	Discharge Modes	105
4.6.1	Direct Current Discharges	105
4.6.2	High Frequency Discharges	111
5	Gaseous Phase and Surface Processes	117
	<i>by H. Frey</i>	
5.1	Elementary Gaseous Phase and Surface Reactions	117
5.1.1	Equilibrium Constant	118
5.2	Gaseous Phase Kinetics	118
5.2.1	Consecutive Reactions of First Order	119
5.2.2	Reactions Moving in Opposite Directions	121
5.2.3	Three-Body Accretion Collisions	123
5.2.4	Three-Body Positive–Negative Ion Recombination	124
5.3	Surface Processes	124
5.3.1	Neutralization of Positive Ions and Emission of Secondary Electrons	124

	5.3.2	Adsorption and Desorption	128
	5.3.3	Fragmentation	131
6		Cathode Sputtering	133
		<i>by H. Frey</i>	
	6.1	Introduction	133
	6.2	Sputtering	133
	6.2.1	Angle Distribution of Sputtered Particles	138
	6.2.2	Sputtering Effects with Single-Crystal Solids	139
	6.3	Coating with Sputtering	143
	6.4	DC Diode Sputtering	143
	6.5	Triode Sputtering	145
	6.6	RF (Radio Frequency) Sputtering	146
	6.7	Bias Sputtering	150
	6.8	Reactive Sputtering	150
	6.9	Magnetron Discharges	152
	6.9.1	Structure	152
	6.9.2	Function of the Magnetron	152
	6.9.3	Estimation of Plasma Density	155
	6.9.4	Discharge Power	156
	6.9.5	Types	156
	6.9.6	Cathodes	157
	6.9.7	Shutters	161
	6.9.8	Infrared Heating	162
	6.9.9	Rate and Film Thickness Measuring Instruments	162
	6.9.10	Two-Chamber Equipment	163
	6.9.11	Multi-Chamber Equipments	164
7		Plasma Treatment Methods	167
		<i>by H. Frey</i>	
	7.1	Plasma Polymerization	167
	7.1.1	Introduction	167
	7.1.2	Physics and Chemistry of Plasma Polymerization	168
	7.2	Plasma Diffusion Treatment	171
	7.2.1	Description of the Method	171
	7.2.2	Fundamental Processes	172
	7.2.3	Correlations Between Different Plasma Parameters	173
	7.2.4	Plasma Nitration of Titanium	174
	7.2.5	Plasma Nitration of Aluminium	174
	7.3	Plasma Spraying	175
	7.3.1	Process Variants	176
8		Particle Beam Sources	181
		<i>by H. Frey</i>	
	8.1	Introduction	181
	8.2	Basic Processes of Ion–Solid Interaction	182
	8.2.1	Loss of Energy	182

8.2.2	Range Distances	185
8.2.3	Collision Cascades and Radiation Damage	186
8.2.4	Ion Mixing	187
8.2.5	Irradiation Amplified Diffusion	187
8.2.6	Surface Texture and Growth Mode	188
8.2.7	Density and Stress	190
8.2.8	Phases in Material Films	191
8.3	Particle Beam Sources	192
8.3.1	Ion Beam Generation	192
8.3.2	Large Area Sources	198
8.4	Application Areas of Ion Beams	204
8.4.1	Primary Ion Beam Deposition (PIBD)	205
8.4.2	Secondary Ion Beam Deposition (SIBD)	206
8.4.3	Ion Beam Etching (IBE, Reactive RIBE)	206
8.5	Ion Implantation	206
8.5.1	Introduction to Implantation	206
8.5.2	Devices for Ion Implantation	217
8.5.3	Pulse Implantation	219
8.5.4	Ion Beam-Assisted Deposition	221
9	Chemical Vapor Deposition (CVD)	225
	<i>by H. Frey</i>	
9.1	Introduction	225
9.2	Physicochemical Bases	226
9.2.1	Initiator Molecules	229
9.2.2	Transportation Phase	234
9.2.3	Deposition and Layer Generation	239
9.3	Equipment for CVD Processes	244
9.3.1	Batch Reactors with Operating Points Within the Kinetically Controlled Range	244
9.3.2	Reactors Operating Within the Mass-Transport Controlled Range	245
9.4	Plasma-Enhanced Chemical Deposition from the Gaseous Phase (PECVD)	246
9.4.1	Deposition of Amorphous Silicon (a-Si:H)	247
9.5	Photoinitiated Vapor Deposition	250
9.5.1	Advantageous Features of PICVD	251
10	Physical Basics of Modern Methods of Surface and Thin Film Analysis	253
	<i>by H. Frey</i>	
10.1	Introduction	253
10.2	Ion Spectroscopes	254
10.2.1	Ion Backscattering	254
10.2.2	Secondary Ion Mass Spectrometry (SIMS)	258
10.2.3	Neutral Particle Spectrometry	262
10.2.4	IPP (Ion-Induced Photo Production)	263
10.2.5	PIXE (Particle-Induced X-Ray Emission)	264

10.3	Electron-Spectroscopic Methods: Auger Electron Spectroscopy (AES) and X-Ray Photoelectron Spectroscopy (XPS)	265
10.3.1	Auger Electron Spectroscopy (AES)	267
10.3.2	ESCA (Electron Spectroscopy for Chemical Analysis), X-Ray Photo Electron Spectroscopy (XPS)	268
10.3.3	UPS (Ultraviolet Photoelectron Spectroscopy)	270
10.4	Inverse Photoemission	271
10.5	Electron Energy Loss Spectroscopy	273
10.6	Diffraction of Slow and Fast Electrons	273
10.7	Image Methods	274
11	Insitu Measurements	279
	<i>by H. Frey</i>	
11.1	Determination of Film Thickness by Resistance Measurement	279
11.2	Rate Measurement by Particle Ionization and Excitation	280
11.2.1	Introduction	280
11.3	Film Thickness and Rate of Deposition Measurements with Quartz Crystal Oscillators	283
11.3.1	Introduction	283
11.4	Optical Measuring Procedures	287
11.4.1	Introduction	287
11.4.2	Systematics of Optical Measuring of Film Thickness	287
11.4.3	Calculation of Optical Film Systems	290
11.5	Determination of the Film Thickness by X-Ray Emission and X-Ray Fluorescence	294
11.6	Atomic Emission Spectroscopy	296
12	Measurements of Thin Layers After the Coating Process	301
	<i>by H. Frey and T. Helmut</i>	
12.1	Measurements of Thermal Conductivity	301
12.1.1	Introduction	301
12.1.2	Experimental Determination	301
12.2	Electrical Conductivity	301
12.2.1	Definition	301
12.2.2	Methods of Determination	301
12.3	Magnetic Properties	302
12.3.1	Properties of Magnetic Layers	302
12.3.2	Magnetic Anisotropy	303
12.3.3	Characteristics of Magnetization Reversal	304
12.3.4	Magnetic Measuring Methods (Overview)	305
12.3.5	Inductive Methods	305
12.3.6	Mechanical Measuring Methods	306
12.3.7	Optical Measuring Methods	306
12.4	Measurement of Color Characteristics	308

12.4.1	Introduction	308
12.4.2	Colorimetry	310
12.4.3	Color Measuring Instruments	312
12.5	Optical Properties of Thin Films	312
12.5.1	Reflectivity and Transmission	312
12.5.2	Ellipsometry	314
12.5.3	Scattering	319
12.5.4	Color	320
12.6	Spectrometers	321
12.6.1	Grating Monochromators and Spectrometers	321
12.6.2	Fourier Transform Spectrometers	323
12.7	Microscopy	324
12.7.1	Optical Microscopes	324
12.7.2	Electron Microscopy	329
12.8	Permeation	337
12.8.1	Measurement Principles	338
12.9	Mechanical Stresses in Thin Films	339
12.9.1	Introduction	339
12.9.2	Interference Optical Measurement	340
12.9.3	Electrical Measurements	341
12.9.4	Laser Scanning Method	341
12.10	Hardness Measurements	341
12.10.1	Introduction	341
12.10.2	Influence of Measurement Conditions on the Hardness Values	342
12.10.3	Measuring Sets and Their Application	343
12.11	Adhesion	344
12.11.1	Introduction	344
12.11.2	Measuring Instruments and Measuring Methods	345
12.12	Roughness of Solid Surfaces	349
12.12.1	Introduction	349
12.12.2	Definitions	349
12.12.3	Measuring Instruments and Measuring Methods	350
12.13	Measuring of Film Thickness	351
12.13.1	Film Thickness Determination by Particle Emission	351
12.14	Determination of Pinhole Densities	353
13	Nanoparticle Films	357
	<i>by H. R. Khan</i>	
13.1	Introduction to Nanomaterials	357
13.2	Synthesis of Nanoparticle Films	358
13.2.1	Diamond Films Deposited by Chemical Vapor Deposition (CVD) and Pulsed Laser Ablation (PLD) Techniques	358
13.2.2	Magnetic Nanocomposites	359
13.2.3	Disordered Magnetic Nanocomposites ($\text{Co}_{50}\text{Fe}_{50}$) _x (Al_2O_3) _{100-x}	360

13.2.4 Nanostructured Nanocomposites Films of Co and CoFe	366
13.2.5 Nanoparticle Transparent and Electrically Conducting Zinc Oxide Films	368
Index	375

Applications and Developments of Thin Film Technology

H. Frey

Thin films are generally used to improve the surface properties of solids. Transmission, reflection, absorption, hardness, abrasion resistance, corrosion, permeation and electrical behaviour are only some of the properties of a bulk material surface that can be improved by using a thin film. Nanotechnology also is based on thin film technology.

Thin films are used if no low-priced bulk material that corresponds to the required specifications of the material exists.

Examples from optics are: changes of reflection or fitting of the transmission of glass bodies; micro-, nano- and opto-electronics are based on thin film technology.

Thin film technologies are divided into PVD (physical vapour deposition) and CVD (chemical vapour deposition) processes.

PVD processes include:

- High-vacuum evaporation
- Cathodic sputtering
- Ion plating
- Ion implantation
- Ion beam mixing
- Plasma diffusion methods and pulse implantation
- Plasma spraying.

High-vacuum evaporation is used in five different evaporation sources:

- Resistance-heated sources (heated directly or indirectly)
- Electron beam evaporators with water-cooled Cu crucibles or lined crucibles and different deflection angles of the electron beam

- Anodic arc evaporators
- Cathodic arc evaporators
- Induction evaporators.

Figure 1.1 gives an overview of vacuum evaporation methods.

The coating process with most variants is cathodic sputtering (Fig. 1.2).

A special process is ion beam sputtering with charged or neutral particles. Further versions are techniques, with electrons inserted into the charge space.

Closely related to cathodic sputtering are plasma-supported CVD processes. The important difference between cathode sputtering and the CVD method lies in the basic material. The use of CVD processes is limited because the gaseous basic materials are frequently missing and the available materials are often very toxic.

Plasma treatment methods in principle are not part of thin film coating processes. With these processes the surface of the bulk materials determining their properties are changed. Properties in the range near the solid surface can be completely changed by ion implantation.

Vacuum plasma spraying completes the vacuum coating processes. With this technology very fast thick films with a high affinity to O₂, or N₂, such as Ti, Ta, Zr and Cr can be sprayed onto surfaces.

Further progress in thin film technology depends on efficient surface analysis methods, above all in connection with high resolution electron microscopy.

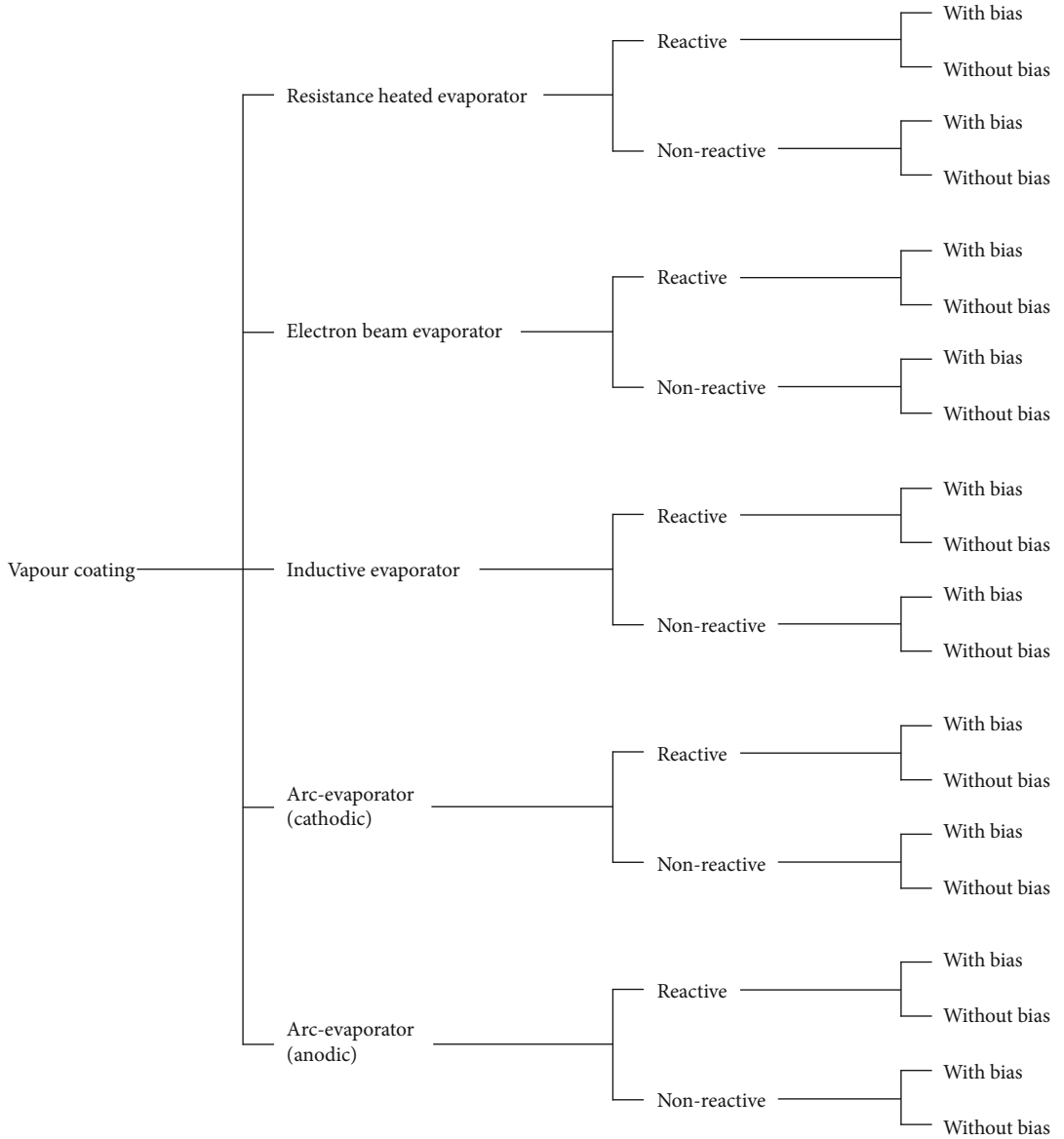


Fig. 1.1 Evaporation in high-vacuum procedure variants

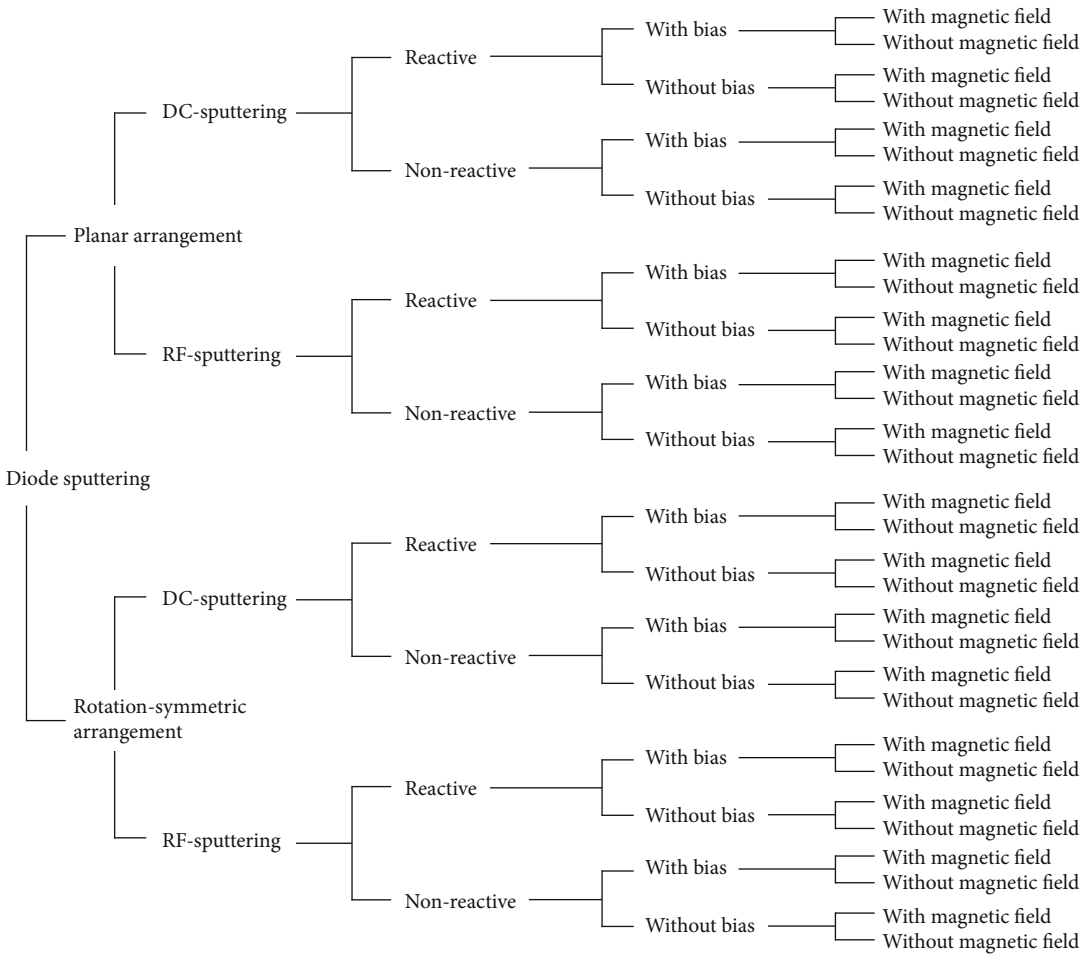


Fig. 1.2 Cathodic sputtering-procedure variants

Relevance of the Vacuum Technology for Thin Film Coatings

2

H. Frey

2.1 Introduction

Vacuum coating processes are characterized by a number of advantages. These include variability of the coating materials, reproducibility of the film properties, and adjustment of the film properties by changing the coating parameters, and the great purity of the coatings. Despite the influence of residual gases in the recipient, and that of the coating material and the condensation rate, the entrapping residual gas molecules into the film can be kept arbitrarily small, if only the residual gas pressure in the recipient is kept accordingly low. Therefore, the conception of the vacuum system during the design and technical execution of vacuum coating plants for Physical Vapor Deposition (PVD) procedures is especially important.

There are many important questions that need to be asked. What is the total pressure necessary, which residual gases are particularly deleterious, and how high can the partial pressure be? Moreover, what is the necessary effective pumping speed of the high vacuum pump in order to achieve within a given time a certain pressure with a still acceptable leakage rate? Further questions are as follows. How large is the gas production during the coating process, how exact must the pressure measurement be, is it sufficient to measure the total pressure, or is it necessary to measure the partial pressure, and which characteristic features of an operating high-vacuum pump are important for a certain coating process? These are only some questions that need to

be answered during the dimensioning of a high-vacuum pump system and the selection of the vacuum equipment [1].

2.2 Influence of Residual Gas on Film Quality

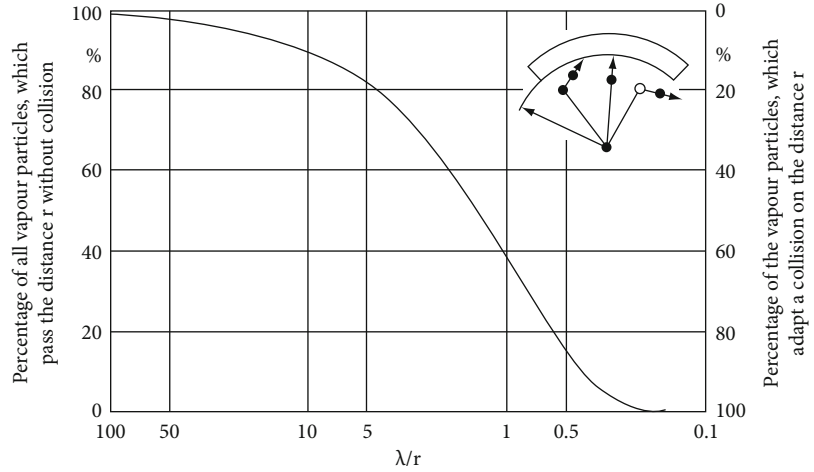
Gaseous impurities can occur on the way from the evaporation source to the substrate surface via collisions of vapour particles with the residual gas particles and when residual gas particles strike the substrate surface. The frequency of collisions increase in volume with the number of residual gas molecules and, therefore, with the pressure in the vacuum chamber.

Since the pressure is inversely proportional to the length of the middle free path, we can say that a vapour particle experiences fewer collisions with residual gas particles, the larger the mean free path is. The mean free path is an important feature of vacuum technology. The mean free path describes the distance that a residual gas atom or molecule on average flies without collision. The mean free path is dependent on pressure, gas species and temperature. For air at a temperature of 20 °C the mean free path is with good approximation:

$$\bar{\lambda} = \frac{6.65 \times 10^{-3}}{p} \quad [\text{cm}] . \quad (2.1)$$

$\bar{\lambda}$ Mean free path [cm],
 p Residual gas pressure [mbar];

Fig. 2.1 Percentage of vapour particles from an evaporation source colliding with residual gas molecules, as a function of λ/r



at 6.65×10^{-3} mbar the mean free path is about 1 cm, at 6.65×10^{-5} mbar 1 m. For electrons the mean free path is around a factor of $4\sqrt{2}$ greater than for atoms.

Figure 2.1 shows the percentage of evaporated vapour particles colliding with residual gas molecules. If the mean free path is approximately as large as the distance between substrate and evaporation source, then ca. 60% of the vapour particles sustain a collision with a residual gas particle. Fortunately, a reaction does not take place at each collision, so that the impurities occurring by collisions in the recipient are actually smaller than what would be expected from Fig. 2.1.

Inert gas particles do not react with other particles. Oxygen and nitrogen, in contrast, react with the evaporated particles. The reaction rate increases if the gas particles are ionized. According to the uncertainties in Fig. 2.1, it is insignificant if the diameter of the vapour molecules, the temperature and the real efficiency of the evaporation source are not known exactly.

With reactive evaporation high collision rates and a high reaction capability of the reaction gas and/or gas mixture are desired. The relationship λ/r should be < 0.5 .

With reactive coating processes the partial vapour pressure and the reaction gas supply are adjusted exactly. The relationship of the two reaction partners can only be determined experimentally, whereby, however, in order to ob-

tain a high condensation rate the partial vapour pressure and therewith the reactive partial pressure must not be arbitrarily high. Otherwise it comes to numerous collisions between high-energy vapour particles and low-energy gas particles. The energy of the particles that condense on the substrate surface is smaller than that of the particles leaving the evaporation source. The results are smooth films with little adhesiveness, whose properties deviate considerably from the bulk material. Therefore, compound generation by reactive evaporating should take place on the substrate surface. The rule generally is: the mean free path of the gas particles corresponds to the distance of the source substrate. At a distance of 30 cm the partial gas pressure should not be larger than 2×10^{-4} mbar. The mean free path is a statistical size.

The impurities from the collision of residual gas molecules on the substrate surface can be estimated as follows:

- For each time unit and square unit on the substrate the striking residual gas molecules can be calculated with the help of following formula:

$$N_R = \frac{n\bar{c}}{4} = 2.63 \times 10^{22} \frac{P_R}{\sqrt{M_r T_R}}. \quad (2.2)$$

In Eq. (2.2) we have

N_R the number the per second and for each square centimetre on the substrate impacted

residual gas molecules in $\text{s}^{-1}\text{cm}^{-2}$,
 p_R the residual gas pressure in mbar,
 M_R the relative molecule mass of the residual gas molecules, and
 T_R the absolute temperature.

The number of N_V ($\text{s}^{-1}\text{cm}^{-2}$) applied for each surface unit of the area and time units on the vapour particle impacting on the substrate surface is

$$N_V = 2.63 \times 10^{22} \frac{p_V}{\sqrt{M_V T_V}}; \quad (2.3)$$

where we have

p_V the saturation vapour pressure of the evaporating material in mbar,
 M_V the relative molecule mass of the evaporating material, and
 T_V the evaporation temperature in K.

The relationship N_V/N_R

$$\frac{N_V}{N_R} = \frac{p_V \sqrt{M_R T_R}}{p_R \sqrt{M_V T_V}} \quad (2.4)$$

is a value for the impurities resulting from the condensation of residual gases. For aluminium with a relative molecule mass of $M_V = 27$, an evaporation temperature of $T_V = 1440$ K and an appropriate saturation vapour pressure of $p_V = 10^{-2}$ mbar, a residual gas pressure of $p_R = 10^{-4}$ mbar and a relative molecule mass of the residual gas of $M_R = 29$, Eq. (2.4), is $N_V/N_R = 47$. In the most unfavourable case, if each residual gas particle striking the substrate surface is adsorbed and reacted with a residual gas particle, a residual gas particle is allotted to 47 aluminium atoms.

With a reduction in the residual gas pressure or an increase in evaporation temperature, drastic improvements of the purity are possible. Since the evaporation temperature is limited, a reduction of the residual gas pressure often remains the only possibility. The probability that a residual gas molecule is received with each impact connection is clearly under 1.

In principle these estimations also apply to for operation of cathodic sputtering equipment. The following must be considered:

a) Conventional sputtering uses total pressures of up to maximum 2×10^{-2} mbar, which is

too high for the operation of some kinds of vacuum pumps. The necessary flow control valve decreases the effective pumping speed at the recipient port and equally increases the residual gas partial pressure.

b) At the beginning of the sputtering process there is increased gas pressure for a limited time due to collisions of high-energy or ionized particles, which is particularly important with throttled pumping speed.

c) When noble gas is fed into a sputtering plant a certain portion of other gases always flows into the recipient. When designing a vacuum pump system and with the requirement of a certain degree of purity of the noble gas it should be considered that it has little propose to choose an extremely high degree of purity and to permit a relatively high residual gas and partial pressure at the same time under a too high leakage gas flow or a too small pumping speed.

A noble gas with 0.01 % impurities would lead to a sputtering pressure of 10^{-2} mbar, without consideration of the possible gettering of residual gas at a partial pressure of 10^{-6} mbar. This is irrespective of the pumping speed of the installed vacuum pump system. In the same order of magnitude, also the partial pressure may be appropriate for that at residual gases, due to the equation

$$p = \frac{Q}{S_{\text{eff}}}, \quad (2.5)$$

where Q is the accumulation of gas by desorption and leakage and S_{eff} the effective pumping speed at the recipient port.

2.3 Generation of Vacuum

The pressure range in which vacuum coating plants operate extends from approximately 10^{-2} mbar into the ultra-high vacuum range. The initial pressures before the coating process begins are generated, in principle, by pump combinations, since there is no single pump that is able to pump down a recipient between the atmo-

spheric pressure and the ultra-high vacuum. To maintain an operating pressure a pump is sufficient when the pumping speed is based on sorption or condensation (ion getter pumps, cryogenic pumping). The operating mode pressure range and characteristic specifications of vacuum pumps are described in detail in books on vacuum engineering [2, 3].

For many years, the pump combination – oil diffusion pump–oil-sealed rotating-vane pump – was the only possibility to create high vacuum on industrial scale. This combination is still often used today for vacuum coating plants, in particular for evaporating plants.

Advantages of this pumping combination are a constant pumping speed below approximately 10^{-3} mbar and a low dependence of the pumping speed on the type of gas. Pumping speeds from some 10 to 100,000 l/s are available. The unfavourable backstreaming of oil steam in the recipient, which leads among other things to impurities and causes degradation of the adhesive strength of thin films, can be reduced by different methods.

Relatively small backstreaming of oil steam and decomposition products from oil diffusion pumps is reached with high-quality pump fluids at ambient temperature pressures of about 10^{-10} mbar. A cooled top baffle nozzle decreases pump backstreaming by an order of magnitude. The additional installation of a baffle with water cooling, refrigerators or LN_2 , results in a further reduction of pump backstreaming.

At pre-evacuation by an oil-sealed rotating-vane pump low-grade oil can get into the diffusion pump and afterwards into the recipient. The quantity of oil diverted in the high vacuum range depends on the contra gas flow and it is the larger, when the residual gas pressure in the volume between diffusion pump and the oil-sealed rotary pump is lower. A pre-evacuation of the recipient over a bypass should, therefore, also not last longer than absolutely necessary.

By gas flushing [4] or installation of a sorption trap oil backstreaming can be decreased drastically, without the pumping speed of the pump used for the pre-evacuation being throttled considerably.

Independently of the type of pre-vacuum pump, because of the extreme loads of the oil in the gasket, oil free pre-vacuum pumps are specially important, e.g. in the semiconductor industry. The oil must possess not only the usual properties like low vapour pressure, small temperature dependence of the viscosity, tight fraction and good lubrication properties, but it also must be stable at high temperatures, inert against chemical attack, e.g. by means of acids, bases and halogens, inert against strong oxidizing agents (oxygen, fluorine), safe when pumping gases with high O_2 -concentrations. In addition to lubrication and sealing, the oil also performs the function of filling dead volume, thus increasing the compression ratio. According to on the requirements, different oils are used.

Maintenance of oil-sealed vacuum pumps requires safety arrangements. Cleaning of contaminated oiled parts, removal of dangerous gases and dangerous sludge is not without risk for the maintenance staff. Oil-free pre-vacuum pumps are suitable as pre-pumps for application in the semiconductor industry. They are combined mainly with turbo-molecular pumps. Oil-free operation of vacuum pumps consists of several single pumps with different rotor profiles, arranged one behind the other. On the high pressure side several pairs of rotors are adjusted in series on a common shaft.

The principle of the pump is shown in Fig. 2.2. The two rotors contained in each stage turn, moving in opposite directions in the volumetric displacement. They periodically open and close the inlet and exhaust ports. The rotors separate the pump chamber. On one side of the rotors the gas is sucked in, on the other it is compressed.

In Fig. 2.2a, the suction and compression cycles begin. The final space above the rotors is reduced, that gas is compressed. At the same time, the right rotor begins to open the inlet port, gas is sucked in. In Fig. 2.2b, the left rotor begins to open the exhaust port, and the compressed gas is transported out. In Fig. 2.2c, the compression and sucking procedures are terminated. Inlet and exhaust ports are closed. After the passage of the rotors to the neutral position, both procedures begin again. Generally, oil-free fore-pumps consist

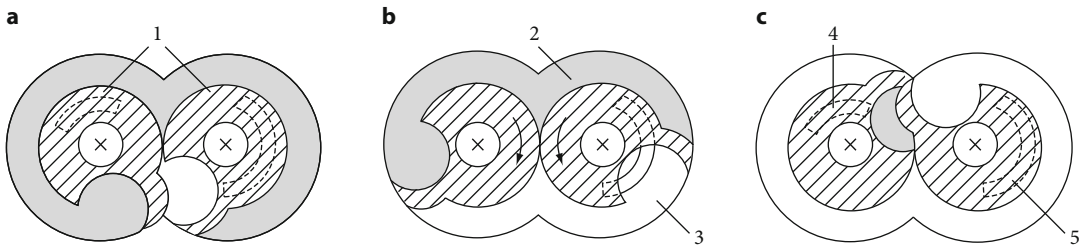


Fig. 2.2 Schematic representation of the pump principle of a claw pump, 1 rotors, 2 compression chamber, 3 suction chamber, 4 exhaust port, 5 inlet port

of four units (claw pumps) that are arranged one behind the other.

A typical pumping speed curve as a function of the intake pressure is shown in Fig. 2.3 [5, 6].

With the vacuum pump combination – turbo-molecular, oil-sealed rotary pump – there is not danger of contamination of the recipient with professional operation. With a high compression ratio for heavy hydrocarbon molecules the partial pressures keeps the hydrocarbons in the recipient without the use of a baffle under the detection limit. Turbo-molecular pumps have small compression and a smaller pumping speed for lighter gases than for heavier ones. While the pumping speed for hydrogen is only lower than 10% for air, the compression capacity is distinguished around nearly six orders of magnitude. Due to the dissociation of water vapour, in vacuum coating equipment a considerable portion of hydrogen develops and the pre-vacuum pump must be large enough to hold it.

The advantages of turbo-molecular pumps are especially suitable for cathodic sputtering equipment. The full use of the pumping speed is a significant process-technical advantage of turbo-molecular pumps, because the residual gas partial pressure is substantially smaller than with other equally large pumps with an upstream throttle valve. The correct dimensioning of pre-pumps is particularly important by higher intake pressure.

The importance of the methods that will in the long run take cryogenic pumping into vacuum coating technology is at present not yet foreseeable. High pumping speed properties and thus fast evacuation times and/or low operating pressures are sufficient reasons for the application

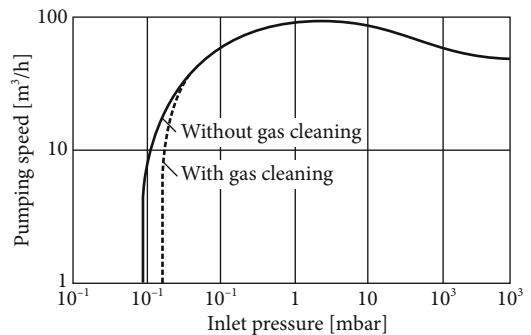


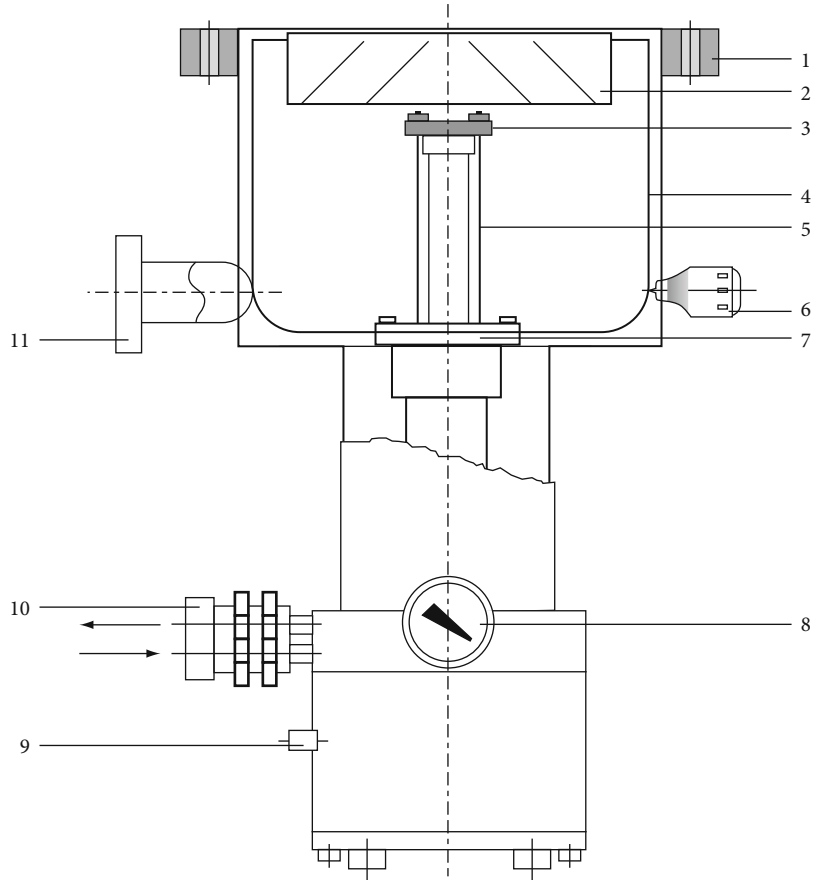
Fig. 2.3 Pumping speed of a four-level claw pump as a function of the intake pressure, _____ without gas flushing, - - - - - with gas flushing

of evaporating plants operated with low residual gas pressures. A clean vacuum with only light gases in the residual gas atmosphere and with high pumping speeds for hydrogen are a further advantage of cryogenic pumping.

For working processes of cathode sputtering plants cryogenic pumping is being increasingly used [7–10]. The refrigerator principle is mainly used for cryogenic pumping. In the range between 10^{-3} and 10^{-2} mbar without interruption, cryopumps can operate for many hours or days before regeneration is necessary.

With two parallel arranged cryogenic pumps an arbitrarily long operating time of cathode sputtering equipments is possible. Modern cryogenic pumps for sputtering equipment are equipped with a cooled baffle (Fig. 2.4). The angles of inclination of optically opaque baffle surfaces are adjusted in such a way that the pumping speed for the discharge gas, normally argon, is usually only throttled at the absolutely necessary degree.

Fig. 2.4 Schema of a refrigerator cryopump.
 1 high-vacuum flange,
 2 baffle, 3 cold stage, 4 radiation shield, 5 pumping surface, 6 safety valve, 7 cold stage, 8 vapour pressure manometers, 9 electrical supply, 10 gas supply, 11 pre-vacuum flange



The high pumping speed for water vapour remains constant with an arbitrary position of the throttle openings.

2.4 Vacuum Measurement

Currently, the range of thin film technology extends to about 19 orders of magnitude of pressure below atmospheric pressure. Consequently, vacuum measuring techniques have had to be developed to measure low pressures of widely differing magnitudes, from a few mbar to about 10^{-16} mbar. There is no single gauge that is able to cope with such a range, although it is the ideal of scientists and engineers to develop such a gauge. For pressure measurement in partial adjustment ranges, a row of different physical principles exist for vacuum measuring with different characteristics [11].

For the use in vacuum coating equipment essentially four types of gauge are of interest:

- a) Thermal conductivity gauge
- b) Friction vacuum gauge
- c) Ionization vacuum gauge with independent discharge (Penning vacuum gauge)
- d) Ionization vacuum gauge with dependent discharge (with hot cathodes).

2.4.1 Thermal Conductivity Gauge

Thermal conductivity gauges are based on a filament mounted in a glass or a metal envelope attached to the vacuum system; the filament being heated by the passage of an electric current. Attainment of the temperature of the filament depends on the rate of supply of electrical energy, heat loss by conductivity through the surrounding gas, heat loss due to radiation (and convection),

and heat loss through the support leads to the filament.

The measurable range of thermal conductivity vacuum gauges for technical operation extends from 10^3 to 10^{-3} mbar. Measurement with thermal conductivity gauges is gas species-dependent, and the accuracy of measurement is different in the partial adjustment ranges. In vacuum coating equipment thermal conductivity vacuum gauges serve for pressure monitoring during the pre-evacuation.

2.4.2 Friction Vacuum Gauge

The measuring element of a friction vacuum gauge is a small steel ball, which rotates in a magnetic field. The pressure is determined from the pressure-dependent deceleration of the steel ball. Since the deceleration can be determined physically, an additional calibration of commercial devices is unnecessary.

In the range between 10^{-2} and 10^{-7} mbar there exists a linear dependency in the range between 10^{-2} and 1 mbar, where a correction factor must be used. The unlimited life cycle, good long-term stability and high measuring accuracy within the pressure range, suggest a broad use of friction vacuum gauges in the future.

2.4.3 Cold Cathode Ionization Vacuum Gauge

With many coating processes that are operated in high vacuum, a very exact pressure measurement is unnecessary. In order to reach a continued high quality of the coated films, it is often sufficient to know whether the residual gas pressure before the start of the coating process lies below an experimentally determined limit pressure. Typical examples are plastic foil coating, vapourization of plastic formed components and production of metallic mirrors. For such applications, cold cathode ionization vacuum gauges are suitable.

Measuring errors are attributed mainly to the pressure-dependent discharge current generated partially by secondary electrons, which are released by gas ions striking the cathode. The

number of excitation and ionization processes releasing secondary electrons not only depend on the pressure, it also depends on the surface property of the cathode. Contamination, therefore, leads to incorrect measurements. The measuring range of commercial devices extends from 10^{-2} to 10^{-7} mbar, which is possible with specifically created gauges.

2.4.4 Hot-Cathode Ionization Gauge

With some coating processes the exactness of the measurements of cold cathode ionization vacuum gauges is not sufficient to achieve an acceptable reproducibility of the film characteristics. Ionization vacuum gauges with hot cathodes can then be used. Hot cathode ionization gauges use the thermionic emission of a cathode, the emitted electrons being accelerated by the electrostatic field through a grid set at a positive potential relative to the cathode. With exact pressure measurements the physical characteristics of the process gas must be considered.

2.4.5 Total Pressure Measurement in Coating Processes

2.4.5.1 Conventional Cathode Sputtering

Conventional sputtering equipment works with total pressures in the order of 10^{-2} mbar, thus in the limits of the measuring range of cold cathode ionization vacuum gauges and thermal conduction vacuum gauges. Already small pressure fluctuations lead to changes of the sputtering rates and thus to deviations from the desired film thickness. Generally, therefore, actual ionization vacuum gauges with hot cathodes are used with such applications. Friction vacuum gauges or gas-sort-independent measuring diaphragm vacuum gauges with capacitive pressure sensor are also assigned.

2.4.5.2 Reactive Cathode Sputtering

The feed of reaction gas to the noble gas that causes the sputtering effect is very small. With the reactive sputtering process of oxide coatings a too-high feed of oxygen leads to oxidation

of the target surface. This, in turn, leads to a drastic decrease of the sputtering and/or condensation rate, film thickness deviations during DC voltage sputtering and changed film properties. With too-low oxygen partial pressure, however, films are part-oxidized and deviate from films with fully-oxidized characteristics. Deviations are also occur if the oxygen partial pressure remains constant and the noble gas partial pressure fluctuates. The gas volume must be kept exactly constant during the coating procedure. This can be achieved production plants by gas flow regulation. Additional precise pressure measurement exercises only control the functioning.

2.4.5.3 Conventional Evaporation

If the residual gas pressure during evaporation in high vacuum is so low that the impurities do not execute a measurable negative influence on the film characteristics, it is completely sufficient not to exceed a given limit pressure during the process cycle. Exact knowledge of the pressure in the recipient is not necessary.

2.4.5.4 Reactive Evaporation

With reactive evaporation, the evaporation speed and/or the condensation rate and the partial pressure of the reactive gas component must be exactly coordinated. Deviations from the standard pressure lead to changes of the film properties. At constant gas flow the pressure is a proportion of the condensation rate and, therefore, it can be used for its regulation.

For precise pressure measurements during reactive coating processes, ionization vacuum gauges with hot cathodes are sufficient. Vacuum gauges with thorium oxide covered cathodes, linearized display and pressure ranges ranging from approximately 1 to 10^{-7} mbar over several decades have a long lifetime and fulfil accuracy requirements.

2.4.6 Partial Pressure Measurement

High purity coatings must be manufactured at a sufficiently low residual gas pressure. Since the

effect of the individual residual gas components is very different, we must have a total pressure measurement with the specifications of the still permissible residual gas pressure. This leads to oversizing of vacuum pump systems.

Moreover, a total pressure measurement is not necessary, if the pressure of additional gas feeding in the recipients is to be kept constant, while the partial pressure of the other residual gases vary more or less strongly. This is not always the case with coating equipment due to the volume of gas fluctuating inside the equipment due to heating during evaporation or by bombardment with particles by sputtering. For gas-species-dependent processes, the use of partial pressure gauges for quantitative recording of all gas components is important for the process cycle.

References

1. Einführung in die Hoch- und Ultrahochvakuumherzeugung. (PDF-Datei; 864 kB) Pfeiffer Vacuum, September 2003
2. Wutz M, Adam H, Walcher W (1988) Theorie und Praxis der Vakuumtechnik. Vieweg, Braunschweig, Wiesbaden
3. Wuest W (2002) In: Profos P (ed) Handbuch der industriellen Messtechnik. Oldenbourg
4. Tsutsumi Y, Ueda S, Ikewaga M, Kobayashi J (1990) Prevention of oil vapor backstreaming in vacuum systems by gas purge method. *J Vac Sci Tech A* 8(3):2764–2767
5. Wycliffe H (1987) Mechanical big vacuum pumps with an oil-free swept volume. *J Vac Technol A* 5(4):2608–2611
6. Troup AP, Dennis NT (1991) Six years of dry pumping: A review of experience and issues. *J Vac Technol A* 9(3):2408–2052
7. Kienel G, Frey H (1977) Betriebsverhalten einer Refrigerator-Kryopumpe an einer Aufdampfanlage. *Vakuum-Technik* 26(2):48–51
8. Baechler WG (1989) Cryopumps for research and industr. *Vacuum* 37(1/2):21–29
9. Haefer RA (1981) Praktische Ausführung von Kryopumpen. Springer-Verlag, pp 147–217
10. Frey H, Haefer RA, Eder FX (eds) (1981) Tieftemperaturtechnologie. VDI-Verlag, pp 301–310
11. Edelmann C (1998) *Vakuumphysik: Grundlagen, Vakuumherzeugung und -messung*. Spektrum Akademischer Verlag, Heidelberg

3.1 Introduction

PVD (physical vacuum deposition) methods are the following: [1]:

- Vacuum evaporation
- Ion plating
- Cathodic sputtering.

These three techniques are also used in reactive processes for coatings with chemical compounds, as well as molecular beam epitaxy [1–5], which is a variant of vacuum evaporation. With ion implantation [6–10], one can change the properties of solid surfaces without coatings. This is not a coating process.

PVD procedures are divided into plasma supported and not plasma supported processes. Vacuum evaporation in high vacuum is not a plasma supported procedure.

The influence of excited or ionized residual gas or vapour particles on the film growth process and, thereby, on the film properties is very favourable for many applications of thin film technology. We therefore, try to produce charged particles also with evaporation.

a desired evaporation rate is reached. The vapour pressure that develops over a liquid or by sublimation of a solid material, is a function of temperature. If both phases (solid and/or liquid and vapour states) exist side by side in a closed chamber at the same temperature, the equilibrium pressure is called the *vapour pressure* or the *saturation vapour pressure*. In such a state of equilibrium an equal number of atoms of the solid and/or the liquid exchanges into the gaseous phase, as atoms from the gaseous phase condense: the evaporation rate and the condensation rate are identical.

This equilibrium state can realized, e.g. in Knudsen evaporators. With evaporation no ideal conditions are present because the vapour at the lower temperature adjudged substrates, installations and recipient walls condense [11].

The saturation vapour pressure that adjusts over a liquid or a solid as a function of the temperature p_D can be calculated by means of the Clausius Clapeyron equation:

$$\frac{dp_D}{dT} = \frac{\Delta Q_D}{T (V_g - V_{fl})}. \quad (3.1)$$

In Eq. (3.1):

P_D is the saturation vapour pressure,

T the temperature of the evaporation material,

Q_D the heat of vapourization,

V_g the molar volume of vapour,

V_{fl} the molar volume of the evaporating liquid and/or the sublimating solid.

The molar volume in the liquid or solid state is very small in comparison with that of the vapour

3.2 Fundamentals

3.2.1 Evaporation Processes

Evaporation in high vacuum uses evaporation sources to heat up the coating material until a sufficiently high vapour pressure is attained, so that

phase. For the saturation vapour pressure at high vacuum evaporation the laws for ideal gases are applicable. This also takes $V_G - V_{fl} \sim V_G - RT/p_D$ from Eq. (3.1),

$$\frac{dp_D}{p_D} = \frac{\Delta Q_D dT}{RT^2} \quad (3.2)$$

or

$$\frac{d(\ln p_D)}{d\left(\frac{1}{T}\right)} = \frac{-\Delta Q_D}{R}. \quad (3.3)$$

The reduction of the vapourization heat with increasing temperature is so small in the range interesting for the evaporation process that it can be regarded as constant.

By integration of Eq. (3.3) we obtain

$$\ln p_D = A' - \frac{\Delta Q_D}{RT} \quad (3.4)$$

and

$$p_D = Ae^{-\frac{B}{T}}, \quad (3.5)$$

where

A is an integration constant, and

B is a constant depending on the heat of vapourization and, therefore, on the evaporation material.

In Eq. (3.5), which is valued in good approximation to vapour pressures up to about 1 mbar, there is a characteristic of evaporation technology. Between the respective saturation vapour pressure, the condensation rate and the temperature of the material in the evaporation source there exists an exponential correlation, which means that relatively small variations in temperature lead to relatively large changes of the condensation rate. Vapour pressure values of metals as functions of temperature are listed in detailed tables (Fig. 3.4).

To obtain the derivation the relations one proceeds from the equilibrium that the same number of particles leaving the liquid or solid surface return to the surface. Since the number of particles returning to the surface is an explicit function of pressure, temperature and relative molecule mass, the particles can be calculated from gas-kinetic laws:

$$N = \frac{n\bar{c}}{4} = 26.4 \times 10^{21} \times \frac{p_D}{\sqrt{MT}}, \quad (3.6)$$

where

\bar{c} is the average speed of the vapour particles in cm/s,

n the number of particles per cm^3 ,

p_D the saturation vapour pressure in mbar,

M the relative molecular mass of the evaporating particles, and

T the temperature of the evaporation source in K.

The mass m (in g) of an individual molecule is:

$$m = \frac{M}{L} = 1.66 \times 10^{-24} \times M, \\ L = 602.3 \times 10^{21} \text{ molecule/mol.} \quad (3.7)$$

The unit area evaporating quantity of G that evaporates at each time (in $\text{g cm}^{-2}\text{s}^{-1}$) can also be calculated from Eqs. (3.6) and (3.7):

$$G = 0.044 \times p_D \sqrt{\frac{M}{T}}, \quad (3.8)$$

with

p_D in mbar and

T in K.

The evaporation rates as a function of temperature are listed in Fig. 3.1 for some metals. In practice, the margin of option for the evaporation rate is not very large. Slowing evaporation velocity leads to undesirable reactions with residual gases. Undesirable part-oxidic coatings develop, e.g. in connection with oxygen. If we want to avoid impurities or still hold the impurities within permissible limits in the coatings, the residual gas pressure must be kept accordingly low during the coating process, with relatively slow evaporation.

At too fast evaporation, which means that the vapour pressure over the source is too large, vapour particles collide with each other. They do not arrive without collisions at the substrate surface, a part returns to the evaporation source.

Even more serious consequences of too high temperatures of evaporation sources are the spontaneously formed vapour bubbles. The evaporation material is ejected by splashing out of the evaporation source, which arrives partially also the substrate, which leads to film damage.

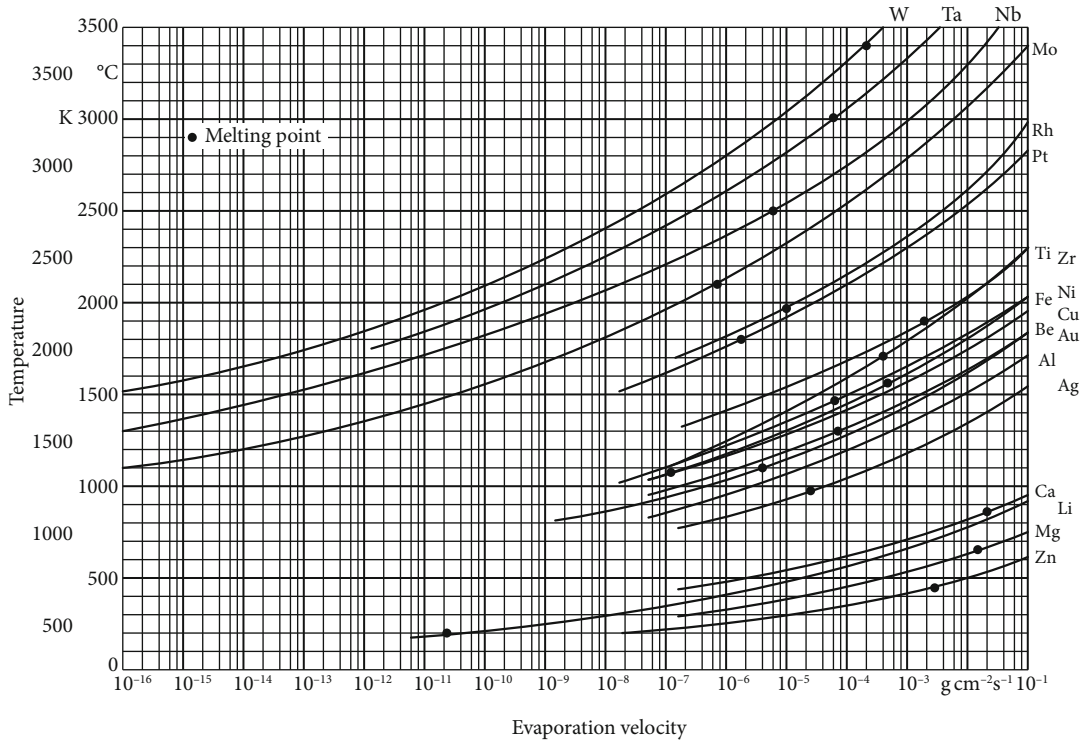


Fig. 3.1 Evaporation rate of metals in the high vacuum range

In practice, vapour pressures are usually in the order of 10^{-2} mbar with evaporation in high vacuum. According to Eq. (3.8) this corresponds, for example, to a relative molecular mass of 100 and a temperature of the evaporation source of 1800 K to an evaporation rate of 10^{-4} ($\text{g}/(\text{cm}^{-2} \text{s}^{-1})$).

An increase of the condensation rate is possible with an enlargement of the evaporating surface. Figure 3.1 also shows that the evaporation rates as a function of temperature change strongly. With zinc as an example, a material that is relatively simple to vapourize, a rise in temperature of approximately 330 to 400 °C leads to an increase of the evaporation rate from 10^{-4} to 10^{-3} $\text{g}/(\text{cm}^{-2} \text{s}^{-1})$, i.e. if the temperature in the indicated range changes by only about 7 °C, the evaporation rate changes about 100 %. In order to increase the evaporation rate of titanium from 10^{-4} to 10^{-3} $\text{g}/(\text{cm}^{-2} \text{s}^{-1})$, the temperature, for example, must be increased from 1560 to approximately 1760 °C.

3.2.2 Transport Phase

The vapour particles emitted from the evaporation source have a mean energy E_D of

$$E_D = \frac{m}{2} v^2 = \frac{3}{2} k T_v = 1.29 T_v \quad [\text{eV}], \quad (3.9)$$

where

m is the mass of a vapour particle in g,

k 8.62×10^{-5} in eV/K,

T_v the temperature of the evaporation source in K, and

v the particle velocity in cm/s.

The energy of the vapour particles depends on the evaporation temperature. The maximum of the Maxwell distribution curve is, for example, at a source temperature of 1500 K at approximately 0.2 eV and at 2000 K source temperature at approximately 0.26 eV, with the assumption that no collisions take place between vapour particles and residual gas particles with lower energy.

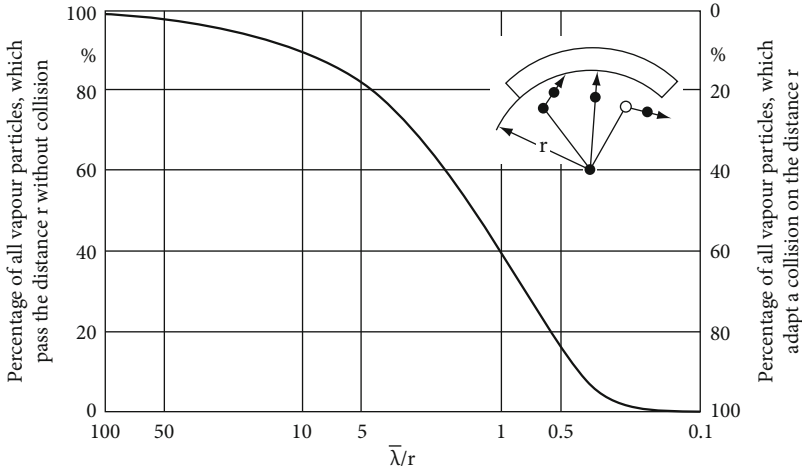


Fig. 3.2 Percentage of outgoing vapour particles at an evaporation source. The vapour particles collide with the remaining gas as a function of λ/r

The two examples show that the energy of vapour particles is relatively low and, therefore, at extremely high evaporation temperatures it also remains low compared to particle energies at sputtering or ion plating. Since for a certain coating material the evaporation temperature may be varied only within close limits, the particle energy is fixed and can be changed only a little.

At higher residual gas pressures the vapour particles transfer energy at each collision to the lower energy residual gas particles, until after sufficient collisions they finally reach energy equilibrium. Then it is valid that

$$E_D = \frac{m}{2}v^2 = \frac{3}{2}kT_R, \quad (3.9a)$$

where T_R is the temperature of the residual gas and/or that of the recipient wall.

At a recipient temperature of 300 K the vapour particles would only have an energy of less than 0.04 eV after many collisions with residual gas particles independently of the evaporation temperature. In the transport phase, molecular compounds can develop through collisions between vapour atoms and residual gas, which lessens the purity of the film.

Figure 3.2 shows the percentage of vapour particles emitted from the evaporation source that collide with residual gas molecules, as a func-

tion of the relationship between the length of the mean free path and the distance between source and substrate.

3.2.3 Condensation Phase

On collision of a vapour particle with the substrate surface the vapour particle possesses a definitive mobility. The particle moves so long on the surface until it takes a fixed place. Since the binding energy of a vapour atom to the substrate is usually smaller than the cohesion energy of the vapour atoms to each other, a vapour atom diffuses – a sufficient energy is pre-supposed – until it meets another vapour atom and finally forms a nucleus. This nucleus formation at the beginning of the coating process preferentially takes place at defects of the substrate surface and first generates islands. By constant growth, the islands grow into one another, until a continuous film develops.

The growth of the nucleus depends on the coating conditions; it prefers high substrate temperatures, a low melting point of the coating material and a low condensation rate. Of particular importance for the film growth process is the energy of the vapour particles, and with plasma supported processes, the constant bombardment

of the surface film by high energy gas molecules or ions.

However, not all molecules that hit the substrate condense. The relationship of the condensing vapour particles to the striking vapour particles is called the *condensation coefficient*. The critical condensation temperature can be shifted to higher temperatures by increasing the vapour beam density. We can also reach a similar effect by applying an intermediate film, the so-called *seed film*. The limit temperatures for progressive condensation are quite different, depending on the material combination.

According to experience, substances with a high boiling point condense better than those with a low boiling point. According to a rule of thumb, for coating materials whose boiling point lies above 1500 °C, one can assume that the condensation coefficient at room temperature is almost 1.

Above the critical condensation temperature at a solid surface, a vapour beam is reflected. One uses this effect, for example, for evaporation from top to bottom, by providing an evaporation source with a heated roof, by which the vapour beams are directed in the desired direction.

3.3 Evaporation of Different Materials

3.3.1 Chemical Elements

With evaporation of a substance heated in high vacuum, the area-specific evaporation rate after Langmuir [12] is

$$\alpha_{v1} = \alpha \times 4.4 \times 10^{-4} \times p_s \sqrt{\frac{M_D}{T}}, \quad (3.10)$$

where

α is the coefficient of evaporation (for ideal evaporation it is $\alpha = 1$),

α_{v1} in $\text{g}/(\text{cm}^2 \text{ s})$ the surface-related evaporation rate,

p_s in 10^{-2} mbar the saturation vapour pressure at the temperature T ,

M_D the mass of the evaporation material, and

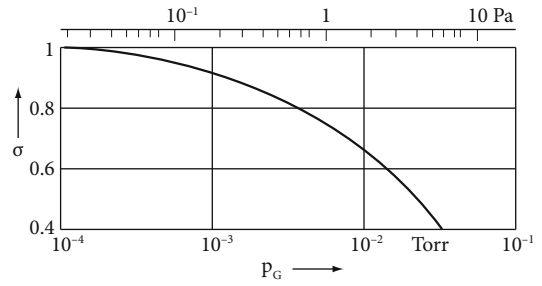


Fig. 3.3 Transmission coefficient τ as function of the gas pressure p_G at the evaporation of copper. Residual gas: air, $p_R < 10^{-4}$ mbar; process gas: argon; vapour pressure over the melt: $p_D = 0.01\text{--}0.03$ mbar, $\alpha_{v1} = 3.2 \times 10^{-4}$ $\text{g}/(\text{cm}^2 \text{ s})$ with $p_R < 10^{-4}$ mbar, α_{v1} and α_{v2} determined by weighing by difference

T the absolute temperature of the evaporated material in K.

Equation (3.10) is valid under the condition that an evaporated molecule is not backscattered through gas or a vapour cloud over the evaporator on the vapour-emitted surface. If this assumption is not applied, then the surface-related evaporation rate α_{v2} is reduced by the factor τ :

$$\alpha_{v2} = \alpha_{v1} \tau. \quad (3.11)$$

τ is a transmission coefficient and can take values between 0 and 1, depending upon the rate α_{v1} and the gas pressure p_G (Fig. 3.3). A gas pressure of 0.01 mbar already has a substantial influence on the evaporation rate α_{v2} .

To calculate the evaporation rates empirically determined values of the vapour pressure must be used. The saturation vapour pressure depends on the temperature as follows:

$$p_s = K_1 e^{-K_2/T}, \quad (3.12)$$

where K_1 and K_2 are material-dependant data from Fig. 3.4. For aluminium, the saturation vapour pressure rises from 0.01 to 0.1 mbar if the temperature increases from approximately 1400 to 1500 K. The saturation vapour pressures for aluminium are reached at temperatures between 500 and 600 K over the melting point. Tungsten has a similar saturation vapour pressure at temperatures between 3600 and 3900 K, i.e. at

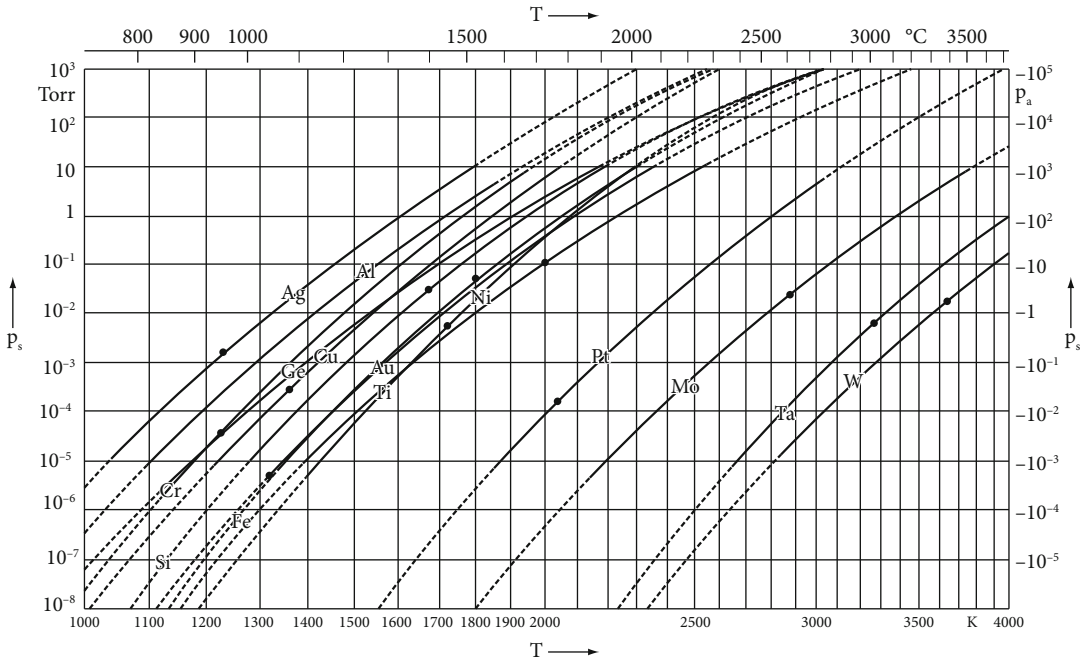


Fig. 3.4 Saturation vapour pressure p_s of some elements in the temperature range between 1000–4000 K

temperatures within the range around the melting point.

The surface-related evaporation rate α_{v1} is with Eq. (3.12)

$$\alpha_{v1} = \alpha \times 4.4 \times 10^{-4} K_1 \sqrt{\frac{M_D}{T}} e^{-K_2/T}. \quad (3.13)$$

Because of the temperature dependence on the saturation vapour pressure, the evaporation rate also grows exponentially with the evaporation temperature (Fig. 3.5). For technical purposes of coating, evaporation rates must be in the range of 10^{-5} to 10^{-2} g/(cm² s¹). The curves in Fig. 3.5 show that generally evaporation from the molten phase must take place in order to achieve the required rates. Only in special cases can the evaporation from the solid state, which means via sublimation, take place.

Impurities, like oxides and carbides, whose density is smaller than that of the evaporation material, occur by melting the vapour delivery surface and partly covering it. Thus the evaporation rate is reduced. Such disturbances do not occur if the impurities have high vapour pressure,

if the impurities thermally decompose or if the vapour can diffuse through the impurity. The high surface temperature due to direct electron beam heating stimulates the thermal decomposition of disturbing films on the melt. By use of evaporation material of high purity and evaporation from water-cooled crucibles, the influence of impurities on the evaporation rate can be kept small.

3.3.2 Alloys

If alloys are to be manufactured, a constant composition from the components on the entire substrate surface and over the film thickness is necessary. The evaporation of alloy films essentially takes place according to two principles: multi-crucible and single-crucible evaporation (Fig. 3.6).

During multi-crucible evaporation [13–15] the components evaporate separately from several crucibles, to which the number of components corresponds. The components condense together on the substrate surface. During single-crucible

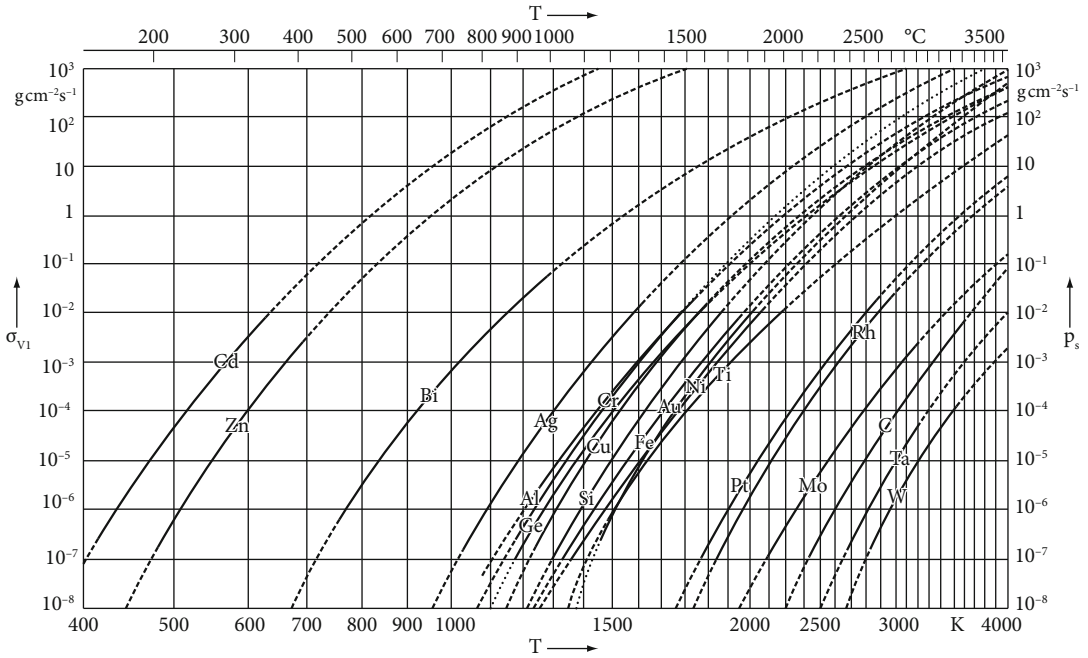
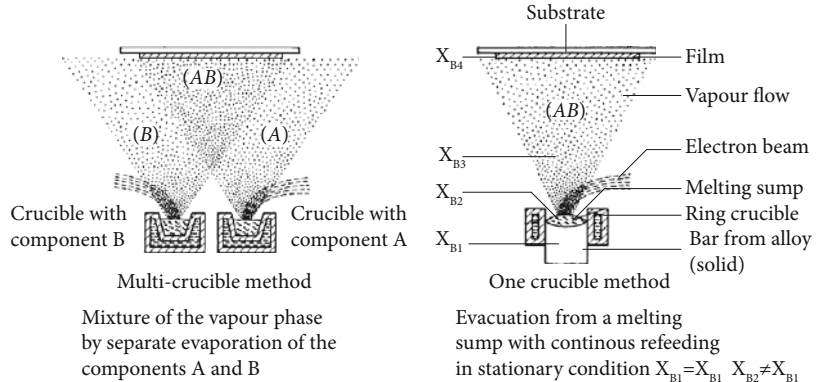


Fig. 3.5 Surface-related evaporation rate α_{v1} of some elements within the range 400–4000 K

Fig. 3.6 Principles for evaporation in the film of alloys with defined composition (example for a binary alloy AB, $X_B \dots$ part of component B in percentage by mass)



evaporation a vapour stream with the composition required for the film is produced and condensed on the substrate surface. A variant of single-crucible evaporation comes from a melt that continues after charging the composition with evaporation properties from a required alloy at the film [16].

3.3.2.1 Multi-Crucible Evaporation

Multi-crucible evaporation can be described by the example of the binary alloy AB with the components A and B. Over the two crucibles

separate vapour streams develop, with the evaporation rates $\alpha_{vA} = \alpha_{vA}(M_A, T_A)$ and $\alpha_{vB} = \alpha_{vB}(M_B, T_B)$ in accordance with Eqs. (3.10) and/or (3.13).

M_A and M_B are the masses of the components A and B and T_A and T_B the temperatures of the vapour delivery surfaces. If the crucibles are arranged at a distance l from each other, whereby l is small against the distance h_V between the substrate and the crucibles, then an expanded range results, in which the vapour stream contains both components of the alloy.